Modelling missile impact and explosion by a finite/discrete element gas-solid interaction

S. Mohammadi
Department of Civil Engineering, University of Tehran, Iran

Abstract

Engineers consider an explosion as a rather wild phenomenon and too complex to be analyzed by deterministic approaches. In this study, however, an attempt has been made to adopt a combined finite discrete element methodology to couple gas dynamics equations and solid deformation states to develop a numerical tool for simulation of explosion. The method uses a standard finite element method accompanied by strain softening behaviour for modeling initiation and propagation of solid cracks due to high gas pressure. This variable high pressure is governed by gas mass and momentum conservation equations. Gas behaviour is fully coupled by solid deformation which changes the density and porosity required in gas dynamics equations. The proposed model for the flow of the detonation gas enables us to evaluate the spatial distribution of the pressure and mass of the detonation gas over a complex geometry of cracked/fragmented solid model. Geometric and material nonlinearities are allowed for fully deformable finite element mesh and cracked/fragmented discrete elements. Local adaptive remeshing (enrichment) techniques are used to geometrically simulate the cracks.
Keywords: impact, explosion, coupled gas solid interaction, finite/discrete element method.

1 Introduction

Accurate and efficient simulation of a missile impact and explosion problem requires a powerful numerical tool for modelling contact, impact, penetration and explosion phenomena. Having involved various mechanical behaviors in various fields such as plasticity, fracture mechanics, gas dynamics and chemical/mechanical behaviour of detonation and explosion has made the numerical modeling of an intact or fractured medium subjected to explosive loading as one of the most difficult engineering simulations.

A strong coupling exists between the gas and solid phases. Detonation causes a phase change of the explosive material into a gas with high pressure and temperature. Part of the amount of release of energy of the solid explosive material is transmitted to the solid mass and causes subsequent deformation, acceleration, fracture and fragmentation of the solid material. Gas expansion and its flow within the crack openings as well as the energy consumption for solid deformation reduce the gas pressure.

The simplest gas pressure-solid deformation model was based on a user defined pressure-time curve, lacking any interaction phenomena [1]. A simple but more sophisticated detonation gas model was proposed by Munjiza [2] which was based on a no gas flow model within a combined finite/discrete element methodology. More recently, a new class of gas flow models have been developed which somehow simulate the gas flow within the crack opening [3, 4].

2 Finite/discrete element modelling of impact/explosion

In order to develop a reliable and efficient numerical approach for the analysis of explosion, a relatively complex interaction algorithm is proposed which adopts two independent meshes for the analysis of solid and gas phases. The equations of gas phase in a porous medium are used to compute the pressure, mass transfer, energy and expansion of the gas at each specified point. The solution for the solid phase will be performed based on the derived gas pressure loading using a finite/discrete element methodology [5, 6]. The proposed algorithm allows for corporation of new lines/edges/bodies created from fracturing and fragmentation of the original model. A bilinear Rankine strain softening plasticity model is employed for modeling the fracture energy release process during the creation and propagation of cracks [6].

To enforce the impenetrability constraint, a penalty based consistent contact mechanics formulation is adopted where the magnitude and direction of the contact force f^{con} can be determined from the displacement vector $\boldsymbol{u}$, the gap vector $\boldsymbol{g}$ and the penalty parameter α [6]:

$$f^{con} = \alpha g \frac{\partial g}{\partial u} \tag{1}$$

An explicit central difference time integration scheme is the most suitable approach for analyzing high velocity impact causing extensive fracture and fragmentation. To capture the contact/impact impenetrability conditions, very small time steps have to be used. It will ensure the stability requirement of the central difference time integration scheme.

3 Gas-solid interaction

Gas and solid phases may be considered separately or studied within a multi-phase porous medium. Combining the macroscopic mass and linear momentum equations, and neglecting the gravitational acceleration and the relative and solid phase accelerations in comparison to very high pressures, leads to [7]

$$\frac{\partial}{\partial t}(n\rho^g) + div\left[\frac{\mathbf{k}k^{rg}\rho^g}{\mu^g}(-\nabla p^g)\right] = 0 \tag{2}$$

where ρ^g is the intrinsic average density, μ^g is the dynamic viscosity, k^{rg} is the relative permeability parameter, and $\mathbf{k}$ is the permeability tensor of the medium.

In this paper, an interaction algorithm based on a two-mesh model is introduced. Two-mesh models have been previously proposed for solving coupled problems. Munjiza discussed the main steps for solving a gas-solid interaction problem but failed to implement it and only used a simple no gas flow model to solve several blasting problems [2].

The present algorithm uses one mesh for modeling the solid material (S-mesh) and the second mesh is used for modeling the gas phase (G-mesh). At any time t, the G-mesh can be mapped onto the S-mesh, and all necessary data can be transferred from the S-mesh to the G-mesh for evaluation of the gas porosity. The G-mesh is analyzed based on the mechanics of porous media; it is assumed that no solid exists for the gas phase and only the equations of mass and momentum are satisfied. The solid phase contributes the equilibrium equations only through the permeability coefficient $\mathbf{k}$. Beginning with the equation (2) for the gas phase, the boundary conditions can be written as:

$$\rho^g \frac{\mathbf{k}k^{rg}}{\mu^g}(-gradp^g)^T.\mathbf{n} = q^g \qquad on \qquad \Gamma_g^q \tag{3}$$

where q^g is the input mass flow and $n = \{n_x, n_y, n_z\}^T$ is the normal vector. The weighted residual form of (6) and (7) can be written as [8]

$$\int_\Omega \mathbf{W}^{*T}\left\{\nabla^T\left[\frac{\mathbf{k}}{\mu^g}(-\nabla p^g)\right] + \frac{\partial\rho^g}{\partial t} - \right\}d\Omega + \int_{\Gamma_g^q}\overline{\mathbf{W}}^{*T}\left[\frac{\mathbf{k}}{\mu^g}(-\nabla p^g)^T.\mathbf{n} - \frac{q^g}{\rho^g}\right]d\Gamma = 0 \tag{4}$$

where $\overline{W}^*, W^*$ are weighted residual functions. Applying the Green theorem and assuming $q^g = 0$,

$$\int_\Omega (\nabla \mathbf{W}^*)^T \frac{\mathbf{k}\rho^g}{\mu^g} \nabla p^g d\Omega + \int_\Omega \mathbf{W}^{*T} \frac{\partial \rho^g}{\partial t} d\Omega = 0 \tag{5}$$

Following the standard finite element interpolation procedure for field variables, pressure P^g can be defined based on the nodal pressures $\overline{\mathbf{P}}^g$ and the shape functions $\mathbf{N}_p$,

$$P^g = \mathbf{N}_p \overline{P}^g \tag{6}$$

and the weighted residual functions are assumed to be the same as shape functions

$$\mathbf{N}_p = \mathbf{W}^* \tag{7}$$

Therefore, equation (5) reduces to

$$\int_{d\Omega} (\nabla \mathbf{N}_p)^T \frac{\mathbf{k}\rho^g}{\mu^g} \nabla \mathbf{N}_p \overline{\mathbf{P}}^g d\Omega + \frac{1}{\partial t} \int_\Omega \mathbf{N}_p^T \partial \rho^g d\Omega = 0 \tag{8}$$

representing the change of mass in unit time. The final form can then be written as

$$\mathbf{M}_{t+\Delta t} = \mathbf{M}_t - \Delta t \mathbf{H}_t^p \overline{\mathbf{P}}_t^g \tag{9}$$

where $\mathbf{H}_t^p$ is the permeability matrix defined by,

$$\mathbf{H}_t^p = \int_\Omega (\nabla \mathbf{N}_p)^T \frac{\mathbf{K}\rho^g}{\mu^g} \nabla \mathbf{N}_p d\Omega \tag{10}$$

To derive the discretized equations, a square cell G-mesh with shape functions $\mathbf{N}_p$ is adopted:

$$\mathbf{N}_p = 0.25[(1-x)(1-y) \quad (1+x)(1-y) \quad (1+x)(1+y) \quad (1+x)(1+y)] \tag{11}$$

and

$$\nabla \mathbf{N}_p = 0.25 \begin{bmatrix} -(1-y) & (1-y) & -(1+y) & (1+y) \\ -(1-x) & -(1+x) & (1-x) & (1+x) \end{bmatrix} \tag{12}$$

$$d\Omega = a^2 dxdy \tag{13}$$

where a is the size of the square element.

Similar shape functions are used to approximate the variations of density and porosity within the element. After lengthy manipulations, the components of symmetric $\mathbf{H}_t^p$ matrix can be derived, [9]

$$\mathbf{H}_{ij}^p = \frac{1}{360}\boldsymbol{K}^T\boldsymbol{D}_{ij}\rho \tag{14}$$

where

$$K^T = \begin{bmatrix} K_1 & K_2 & K_3 & K_4 \end{bmatrix} \tag{15}$$

$$\rho^T = \begin{bmatrix} \rho_1 & \rho_2 & \rho_3 & \rho_4 \end{bmatrix} \tag{16}$$

and the components of symmetric D matrix,

$$\begin{gathered}
D_{11} = \begin{bmatrix} 48 & 18 & 18 & 6 \\ 18 & 28 & 6 & 8 \\ 18 & 6 & 28 & 8 \\ 6 & 8 & 8 & 8 \end{bmatrix} \quad
D_{12} = -\begin{bmatrix} 18 & 8 & 3 & 1 \\ 8 & 18 & 1 & 3 \\ 3 & 1 & -2 & -2 \\ 1 & 3 & -2 & -2 \end{bmatrix} \\
D_{13} = -\begin{bmatrix} 18 & 3 & 8 & 1 \\ 3 & 14 & 1 & 2 \\ 8 & 1 & 18 & 3 \\ 1 & 2 & 3 & 2 \end{bmatrix} \quad
D_{14} = -\begin{bmatrix} 12 & 7 & 7 & 4 \\ 7 & 12 & 4 & 7 \\ 7 & 4 & 12 & 7 \\ 4 & 7 & 7 & 12 \end{bmatrix} \\
D_{22} = \begin{bmatrix} 28 & 18 & 8 & 6 \\ 18 & 48 & 6 & 18 \\ 8 & 6 & 8 & 8 \\ 6 & 18 & 8 & 28 \end{bmatrix} \quad
D_{23} = -\begin{bmatrix} 12 & 7 & 7 & 4 \\ 7 & 12 & 4 & 7 \\ 7 & 4 & 12 & 7 \\ 4 & 7 & 7 & 12 \end{bmatrix} \\
D_{24} = -\begin{bmatrix} 18 & 3 & 8 & 1 \\ 3 & -2 & 1 & -2 \\ 8 & 1 & 18 & 3 \\ 1 & -2 & 3 & -2 \end{bmatrix} \quad
D_{33} = \begin{bmatrix} 28 & 8 & 18 & 6 \\ 8 & 8 & 6 & 8 \\ 18 & 6 & 48 & 18 \\ 6 & 8 & 18 & 28 \end{bmatrix} \\
D_{34} = -\begin{bmatrix} -2 & -2 & 3 & 1 \\ -2 & -2 & 1 & 3 \\ 3 & 1 & 18 & 8 \\ 1 & 3 & 8 & 3 \end{bmatrix} \quad
D_{44} = \begin{bmatrix} 8 & 8 & 8 & 6 \\ 8 & 28 & 6 & 18 \\ 8 & 6 & 28 & 18 \\ 6 & 18 & 18 & 48 \end{bmatrix}
\end{gathered} \tag{17}$$

Two additional assumptions are required for defining the solid and gas equations of states. The first assumption is the way $V_s(p)$; the volume of a solid at mean pressure p, can be calculated from its volume at zero pressure state $V_s(\text{o})$,

$$V_s(p) = V_s(\circ) * e^{-p/\lambda} \tag{18}$$

where λ is the rate of volume reduction. The second assumption is required to include the effects of high gas pressure and temperature conditions,

$$P = \overline{R}\frac{\rho}{1-\rho e^{-0.4\rho}}T \tag{19}$$

4 Numerical simulations

4.1 Example 1

A concrete plate is subjected to a $V = 30\,{}^{m}\!/_{s}$ foreign object impact. Figure 1 defines the geometry of the problem and shows the initial finite element mesh. Material properties are given in Table 1 [10].

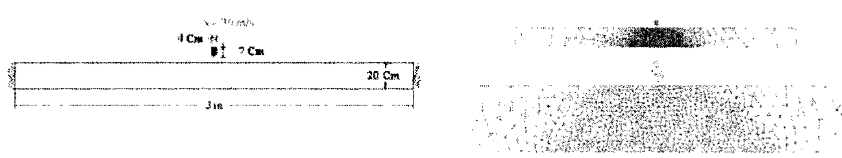

Figure 1: Missile penetration into a ceramic plate, geometry and FE mesh.

Table 1: Material properties.

Concrete plate		Steel impactor	
$E = 23\,GPa$	$\alpha_N = 250GPa$	$E = 2100\,GPa$	$\alpha_N = 15e3GPa$
$\rho = 2500\,{}^{kg}\!/_{m^3}$	$\alpha_T = 250MPa$	$\rho = 7850\,{}^{kg}\!/_{m^3}$	$\alpha_T = 15GPa$
$G_f = 110\,{}^{N}\!/_{m}$	$f_t = 1MPa$	$\nu = 0.3$	

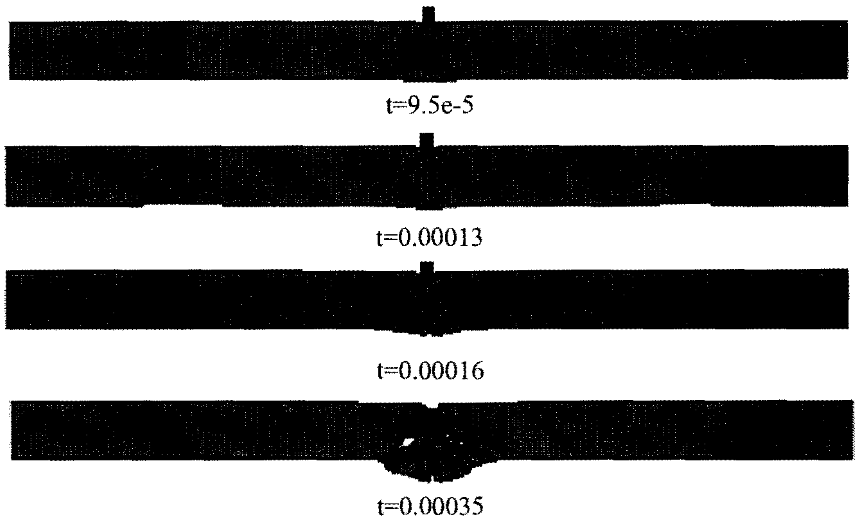

Figure 2: Progressive penetration and fracture patterns.

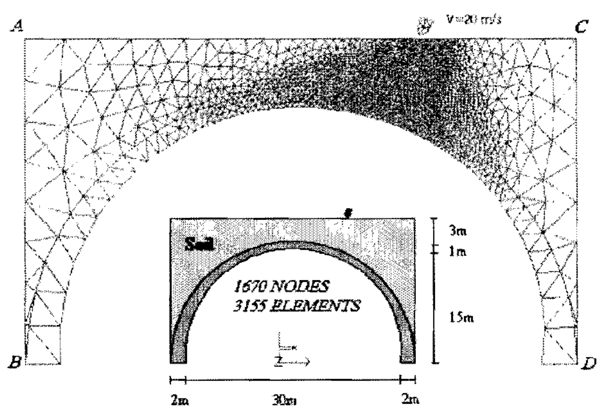

Soil
$E = 40\,\text{MPa}$
$\rho = 1600\,{}^{kg}/_{m^3}$
$\nu = 0.15$
$f_t = 0.1\text{MPa}$
$G_f = 15\,{}^{N}/_{m}$

Figure 3: Missile impact on a subsurface shelter with soil properties.

The results of a finite/discrete element modeling of the problem are illustrated in Figure 2. Extensive cracking is predicted to occur in successive timesteps. The final cone-shaped damage in concrete plate is in well agreement with experimental observations [10].

4.2 Example 2

A subsurface shelter is assumed to be subjected to a missile impact as depicted in Figure 3 [10]. The soil properties are also given in this figure while the concrete and steel missile material properties are similar to example 1.

Figure 4 illustrates the missile penetration patterns, and the extent of soil and concrete shelter failures at various stages of missile impact. The present results can only be achieved if carefully calibrated necessary contact analysis parameters are used.

4.3 Example 3

A $0.33 \times 0.33\ m$ square hole filled with ANFO explosive material is located at the centre of a $1 \times 1\,m$ square block of rock (Figure 5). Properties of rock and explosive material are given in Table 2 [8].

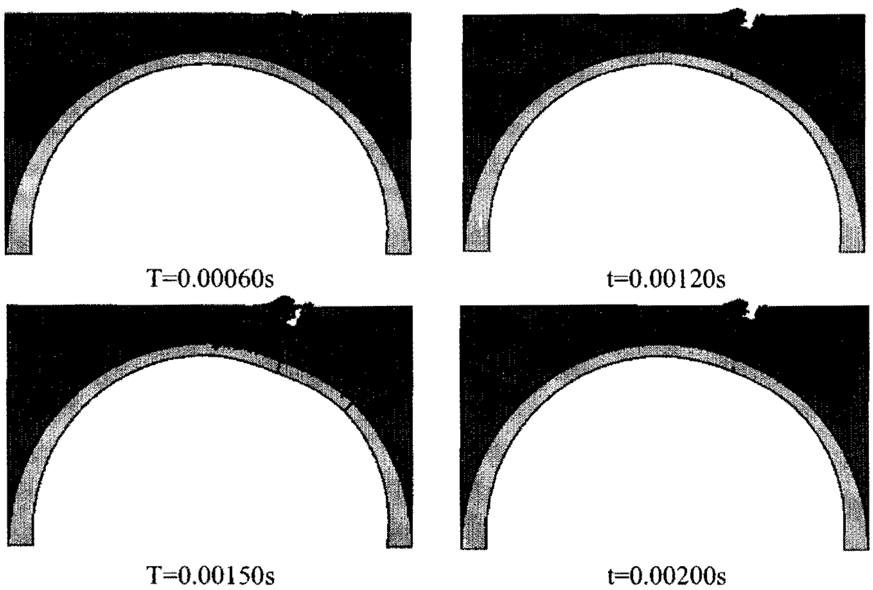

Figure 4: Patterns of missile penetration and soil and concrete shelter failures.

Table 2: Material properties.

Solid		ANFO	
$E = 28000\ _{MPa}$	$G_f = 250\ _{\frac{N.m}{m^2}}$	$VOD = 1725\ _{m/s}$	$\mathbf{K} = 3 \times 10^{-8}\ \frac{m^2}{pa.s}$
$\rho = 4200\ _{kg/m^3}$	$v = 0.1$	$\rho = 850\ _{kg/m^3}$	$Q_e = 3700\ _{\frac{kJ}{kg}}$

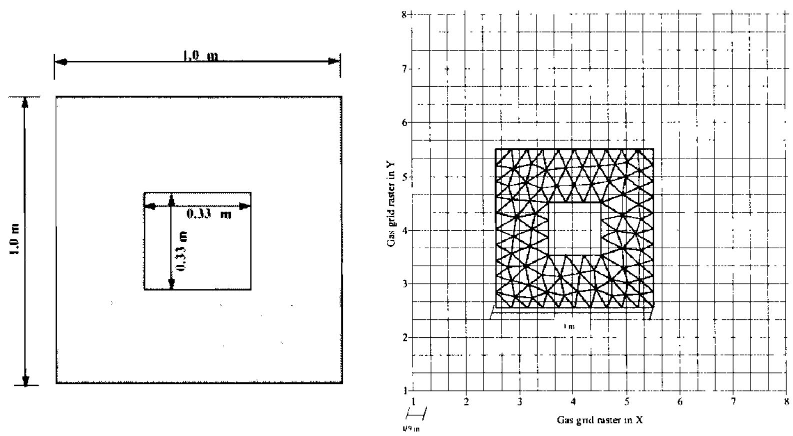

Figure 5: Geometry of the contained explosion problem, and the 2-mesh model.

Figure 6 illustrates the initial two-mesh modeling and the pressure contours and cracking patterns in different timesteps. By increasing the openings of cracks, part of the gas mass is transferred through the openings; instantly increasing the gas pressure in the vicinity of cracks. The pressure substantially reduces immediately after the escape of gas from the crack opening.

It is important to assess the performance of different gas meshes. A very coarse mesh which does not have any point inside the explosion hole (borehole) generates no gas pressure on solid mesh. A finer mesh with only one node of the gas mesh within the explosion borehole generates some gas pressure but gives poor results. Better approximation may be achieved by adopting finer gas mesh. It is important to note that there should be a practical limit on the minimum size of the gas mesh as the cost of numerical simulation may be unacceptably increased with a very small size of the gas mesh.

5 Conclusion

In this paper, a two-mesh coupled gas dynamics/solid mechanics interaction model is developed and implemented into a combined finite/discrete element methodology to simulate the complex behavior of impact and explosion of foreign objects on structures. The solid domain is expected to experience extensive fracture and fragmentation; affecting the pressure and density of the blast induced gas. Several numerical simulations have been used to assess the performance of the proposed algorithm. The method, however, becomes numerically expensive as the size of regular G-mesh is reduced to enhance the accuracy of the gas related computations.

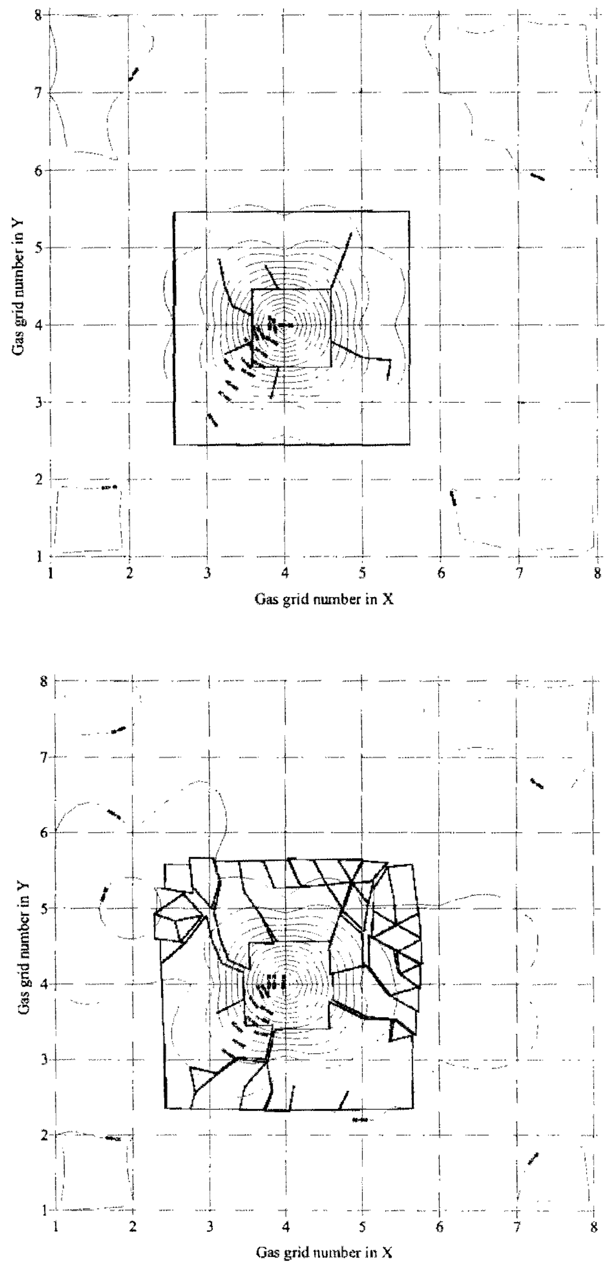

Figure 6: Cracking patterns and gas pressure contours at t=0.0003, 0.001s.

References

[1] Bauer, A.A. & Fratzos, D., Finite element modeling of pre-split blasting using measured time curves. Society of Explosive Engineers Annual Meeting, Miami, USA, 1987.

[2] Munjiza, A., Discrete elements in transient dynamics of fractured media. Ph.D. thesis, University of Wales Swansea, 1992.

[3] Preece, D.S., Burchell, S.L. & Scovira, D.S., Coupled gas flow and rock motion modeling with comparison to bench blast field data. In Proceedings Fragblast-**4**; 239-247, 1993.

[4] Munjiza, A., Latham J.P. & Andrews K.F., Detonation gas model for combined finite-discrete element simulation of fracture and fragmentation". International journal for numerical methods in engineering . **49**:1495-1520, 2000.

[5] Munjiza, A., Andrews, K.R.F. & White, J.K., Combined single and smeared crack model in combined finite-discrete element method. International journal for numerical methods in engineering; **44**: 41-57, 1998.

[6] Mohammadi, S., Discontinuum Mechanics Using Finite and Discrete Elements, WIT Press, UK, 2003.

[7] Lewis, R.W. & Schrefeler, B.A., The Finite Element Method in the Static and Dynamic Deformation and Consolidation of Porous Media. Second edition. England, 1998.

[8] Mohammadi, S. & Bebamzadeh, A., A Coupled Gas-Solid Interaction Model for FE/DE Simulation of Explosion. Finite Elements in Analysis and Design. In press.

[9] Bebamzade, A., Numerical Simulation of Rock Blasting. M.Sc thesis, Department of Civil Engineering, University of Tehran, 2003.

[10] Mahootchian, A., Numerical Simulation Missile Impact and Penetration by a Combined Finite/Discrete Element Method. M.Sc thesis, Department of Civil Engineering, University of Tehran, 2002.